Ultraviscosity in Entangled Polyelectrolyte Complexes and Coacervates

Khalil Akkaoui, Mo Yang, Zachary A. Digby, Joseph B. Schlenoff*

Department of Chemistry and Biochemistry

The Florida State University

Tallahassee, FL 32308-4390 USA

Abstract

The spontaneous association of oppositely charged polyelectrolytes is an example of liquid-liquid phase separation. The resulting hydrated polyelectrolyte complexes or coacervates, both termed "PECs," display a wide range of viscosities. In addition to the usual dependence of viscosity on molecular weight and volume fraction expected for condensed neutral polymers, PECs also contain dense charge pairing between positive, Pol⁺ and negative, Pol⁻, repeat units. These "stickers" slow polymer chain dynamics on multiple length scales. Pol⁺Pol⁻ charge pairs may be broken by the addition of salt to solutions contacting PECs, reducing viscosity ("saloplasticity"). Here, dynamics of matched of polycation, the pairs poly(methacryloylaminopropyltrimethylammonium chloride) PMAPTAC and polyanion, sodium poly(methacrylate), PMANa, with molecular weights considerably above the entanglement concentration, were measured as a function of temperature and salt concentration. The dynamics of NaCl ions in PECs were also determined and correlated to the segmental relaxation times

which control viscosity. A suite of relaxation times corresponding to ion, monomer, Pol⁺Pol⁻ pair exchange, entanglement, and reptation was determined or estimated. The zero-shear viscosity, η_o , was found to be an unusually strong function of molecular weight, with the scaling $\eta_o \sim M^5$. A polymer coil size, measured by small angle neutron scattering, was used in concert with new quantitative expressions to provide a good fit of theory to experiment for this unusual scaling.

Keywords: phase separation, scaling, ion transport, ion-containing polymers, relaxation, dynamics.

*jschlenoff@fsu.edu

Introduction

Physical interactions between molecules occur through a variety of mechanisms, including dipolar interactions, hydrogen bonding, van der Waals, hydrophobic and Coulombic forces. (Bio)macromolecules often rely on multiple or polyvalent interactions to make associations rugged and selective.¹ For example, when polyelectrolytes of opposite charge are mixed, positive and negative repeat units pair and condensed amorphous polyelectrolyte complexes or coacervates, PECs, are formed.^{2, 3} This phase separation of synthetic polymers is related to the liquid phase condensation⁴ thought to be responsible for a host of membraneless organelles found within cells and possibly for the origins of life.^{5, 6, 7}

Polyvalent charge pairing stabilizes higher order structures in proteins (via "salt bridges" between charged peptides⁸) and is used by some organisms to produce bioadhesive, viscous binders.^{9, 10} The amorphous/disordered nature of many biological coacervates makes them the "dark matter" of the cell – important in function but lacking the long-range or periodic structure that would provide diffraction data suggesting structure/function relationships.

The chemistry, biology and physics of coacervating polymers have been probed using tools both specialized to, and shared by, each field. Charge pairing interactions are thought to prevail when biomolecules such as RNA are involved in coacervation. 11, 12 Peptides with other modes of interaction offer additional sequence- and location-dependent mechanisms of association. 13, 14 In order to predict the formation of coacervates, phase diagrams are constructed describing thermodynamic boundaries between condensed and dilute phases. 15, 16, 17, 18 Recent attention has also turned to the *dynamics* of PECs. Using a rough comparison of storage modulus, G', and loss modulus, G'', these studies can be grouped according to whether the PEC is in the more solid-like or liquid-like regime. Additional categories of previous works include whether narrow molecular weight distribution, Đ, fractions were employed and whether polymer chains in

the system were clearly above the concentration and/or molecular weight required for entanglement. Viscoelastic properties of solid-like PECs were measured on broad Đ ultrathin samples that were probably entangled but also close to the glass transition temperature. ¹⁹ Spruijt et al. studied the linear viscoelasticity, LVE, of liquidlike PECs with narrower Đ.^{20, 21} The salt-induced transition between solid and liquid broad Đ PECs²² was examined by Liu et al.²³ and Hamad et al.²⁴ Marciel et al. matched pairs of polypeptides to make liquidlike PECs²⁵ while Huang et al. explored the effect of charge density on the LVE of liquidlike PECs.²⁶ The present study focuses on the dynamics of PECs made from a series of polyelectrolytes with well-defined, matched molecular weights, well into the entanglement regime and well above the glass transition temperature.

Polycations have repeat units Pol⁺ neutralized by counterions A⁻. The repeat units of polyanions, Pol⁻, are balanced with cations M⁺. Most of the driving force for complexation comes from the release of counterions,^{27, 28} an entropic component.

$$Pol^{+}A_{aq}^{-} + Pol^{-}M_{aq}^{+} = Pol^{+}Pol_{pec}^{-} + A_{aq}^{-} + M_{aq}^{+}$$
 [1]

The Pol⁺Pol⁻ charge pairs are considered to be "sticky" interaction points and the material remains well hydrated in aqueous solutions. The density of charge pairs is reversibly controlled by the concentration of salt, MA, solution in which they are immersed.

$$Pol^{+}Pol_{pec}^{-} + M_{aq}^{+} + A_{aq}^{-} = Pol^{+}A_{pec}^{-} + Pol^{-}M_{pec}^{+}$$
 [2]

Equation 2 represents partial reversal of the formation process, Equation 1. Polyelectrolyte chains have very little translational entropy so the PEC ion composition is determined by a Donnan equilibrium between internal and external salt concentration.²⁹ Other ways to vary the charge density within PECs include changing the pH³⁰ or introducing extra charge (e.g. by

phosphorylation^{11, 31, 32}). Generally speaking, the greater the density of charge pairs the more stable the PEC.^{29, 33}

The dynamics of ions within ion-containing polymers are believed to be coupled to the dynamics of polymer segments.³⁴ Complexed polyelectrolytes have a high charge density. Introducing ions into PECs by the "doping" process shown in Equation 2 causes large variations in properties such as ionic conductivity³⁵ and viscoelasticity. The ability to switch on and off multiple interactions between molecules is the basis of salt control of properties, or "saloplasticity." The polyelectrolytes investigated here were recently used to compare a predicted scaling of PEC viscosity with molecular weight.³⁶ However, although a full rubbery plateau was observed in the LVE, chains were not sufficiently long to fully address any scaling of properties with chain length well into the entanglement regime. The present work focuses on polymer chains well above entanglement, and is organized as follows: first, static properties of a PEC are presented, including equilibrium composition and polymer coil size, made from narrow molecular weight distribution polyelectrolytes. There follows a quantitative analysis of counterion dynamics, then of polymer dynamics. A previously unknown regime of polymer viscosity, controlled by multiple weak sticky associations, scaling with the fifth power of chain length, is revealed.

Experimental

Materials. NaN₃, NaNO₃, KBr and NaCl were from Sigma Aldrich. Acetone (99.5%) for polymer fractionation was from VWR Chemicals. Deuterated PMA, D-PMA, from Polymer Source Inc., had a M_w of 387,000, M_n of 365,000 and polydispersity index, Đ, = M_w/M_n, of 1.06. Deuterium oxide (D₂O, Cambridge Isotope Laboratory Inc., 99.9%) was used to prepare ¹H NMR solutions and for samples used in neutron diffraction. Monomers were 3-(methacryloylamino)-propyltrimethylammonium chloride (MAPTAC) (Sigma Aldrich, 50 wt %H₂O) and methacrylic acid

(MAA) (Alfa-Aesar, 99%). All solutions were prepared with deionized water (18 M Ω Barnstead NanoPure).

Polymer synthesis. MAPTAC and MAA were mixed with inhibitor removal beads for 4 h. Free radical polymerization of MAPTAC and MAA was carried using K₂S₂O₈ as an initiator. 385 g of MAPTAC aqueous solution (192.5 g MAPTAC, 0.87 mol) and 0.57 g of K₂S₂O₈ (3 x 10⁻³ mol) were mixed with 350 mL deionized water to give 0.5 M monomer. The solution was purged under N₂ and heated at 65 °C for 12 h under vigorous stirring. 93.5 g (1.09 mol) of aqueous MAA along with 1.32 g (5 x 10⁻³ mol) of K₂S₂O₈ was added to 1.9 L of deionized water to yield a monomer concentration of 0.6 M and the solution was heated at 65 °C under N₂ with stirring for 12 h. The PMAA was neutralized to the sodium salt (PMANa) with NaOH, taking the pH from 3.2 to 9. The polymer solutions were dried at 65 °C under vac for 72 h, and the dry polymer powder collected and fractionated.

Polymer Fractionation. Molecular weight fractionation was used to isolate fractions of the two polyelectrolytes. 50 g PMAPTAC (M_w = 619 kDa, D = 1.35, see Supporting Information Figure S1) was dissolved in 500 mL water and fractionation was carried out through the gradual addition of acetone to the polymer solution. The first fraction was obtained after the addition of approximately an equal ratio of acetone to water, and the cloudy solution was centrifuged at 7000 rpm for 4-5 h to remove the fraction. Acetone was slowly added sequentially and ten fractions of PMAPTAC of decreasing molecular weight and low D were collected and dried at 120 °C. A similar procedure was used to fractionate PMANa (M_w = 357 kDa, D = 1.43, see Supporting Information Figure S2).

Size Exclusion Chromatography (SEC). The weight-average molecular weight, M_w, number-average molecular weight, M_n, and Đ for PMAPTAC and PMANa were determined by SEC. The refractive index increments (dn/dc) reported by Yang et al. for both polyelectrolytes were used.³⁶ Samples with 3.0 mg mL⁻¹ of PMANa or PMAPTAC in 0.3 M NaNO₃ were prepared and filtered

through 0.2 μ m poly(ether sulfone) filters. The mobile phase was 0.3 M NaNO₃ preserved with 200 ppm NaN₃. The injection volume was 50 μ L and the flow rate 1.0 mL min⁻¹. PMAPTAC separations employed a 10 μ m polycation column (300 x 8 mm, PSS Inc. Novema Max Lux analytical 1000 Å) with a 10 μ m PSS Novema Max Lux guard column. PMANa separations used one 17 μ m column (300 x 7.5 mm, Tosoh Biosciences TSK-GEL G5000PW), one 13 μ m column (300 x 7.8 mm², Tosoh Biosciences TSK-GEL GMPWx) and a TSK guard column. The detectors were a calibrated DAWN-EOS multiangle light scattering detector and a rEX refractometer, calibrated with NaCl standards, both from Wyatt Technology. Polyelectrolyte molecular weight data is summarized in Table 1 and Supporting Information Figures S1 and S2.

PEC Formation. PMAPTAC/PMANa fractions were paired according to their chain lengths. 20 mL each of 0.2 M (molar concentrations of all polymers are given with respect to their monomer units) polymers solutions in 1 M NaCl were mixed. The resulting PEC remained dissolved at this [NaCl]. Water was added in 5 mL increments until the PEC precipitated out of solution. The PEC phase separated from the salt solution after the volume of water added brought the [NaCl] to lower than 0.6 M. The solution was centrifuged at 6000 rpm for 2 h to form a clear, continuous macroscopic PEC (coacervate) phase. The dilute phase (supernate) was removed and the PECs (coacervates) were doped at the salt concentration of interest. To ensure equilibration at the various salt concentrations, the solutions were annealed at 60 °C for 12 h then gradually cooled to room temp.

¹H NMR. NMR was used to study the stoichiometry of the PEC to verify the mole ratio PMAPTA:PMA was close to 1:1 (see Table 1 and Supporting Information Figure S3). 10 mg mL⁻¹ of dry PEC was dissolved in 1.0 M KBr in D₂O and ¹H NMR spectra were acquired using an Avance 600 MHz NMR (Bruker).

Table 1. Polyelectrolyte combinations and stoichiometry in PMAPTA/PMA complexes. n_{MAPTAC} and n_{MANa} are the respective degrees of polymerization or number of repeat units for PMAPTAC and PMANa. n_{avg} is the average number of repeat units of polyelectrolyte pairs (**A** thru **E**). N_{avg} is the average number of Kuhn repeat units using a Kuhn length of 1.5 nm. The ratio of the polyelectrolytes in the PEC was obtained using ¹H NMR.

	(MAPT	AC)n	(MANa	1) n	n_{MAPTAC}	n_{MANa}	Navg	N_{avg}	ratio
Pair	M_{n}	$M_{\text{w}}/M_{\text{n}}$	M_n	M_w/M_t	า				
	(kg mol ⁻¹)		(kg mol ⁻¹)						
Α	1040	1.05	516	1.04	4700	4780	4740	796	0.99
В	849	1.06	389	1.05	3850	3600	3730	627	1.01
С	524	1.06	283	1.15	2370	2620	2500	420	0.98
D	346	1.04	136	1.14	1570	1280	1420	239	1.04
E	226	1.05	121	1.08	1020	1120	1070	180	1.02

Rheology. A stress controlled DHR-3 rheometer (TA Instruments) was used to study the linear viscoelastic behavior of the different pairs of PMAPTA/PMA complex doped in 0.01 M NaCl. Samples exposed to a range of [NaCl] (0.01, 0.05, 0.10, 0.15, 0.20 M) were prepared using **Pair B** (n_{avg} = 3730, Table 1). The PECs were transferred onto the bottom plate of the rheometer and compressed 10% using 20 mm parallel plate geometry. During measurements, all PECs were maintained immersed in the corresponding [NaCl] using a reservoir built in-house which was capped to avoid solvent evaporation. Frequency sweeps were performed at temperatures ranging from 0 °C to 85 °C. A ten min delay was applied before every frequency sweep to make sure the PEC had reached the target temperature.

Composition and Kinetics Measurements. Conductivity was used to measure both the doping level of PECs exposed to various [NaCl] and the kinetics of ion release as a function of temperature. PECs were made from the starting solutions (PMAPTAC, M_w = 619 kDa, Đ = 1.35; PMANa, M_w = 357 kDa, Đ =1.43 kDa, see Supporting Information Figures S1 and S2. Đ_{average} ≈ 1.4) prior to fractionation. PEC samples were doped using five [NaCl] (0.01, 0.05, 0.10, 0.15, 0.20 M). The PECs were soaked for 12 h in salt solutions and the solutions replaced with fresh salt solutions of the same concentrations to allow the system to equilibrate to a specific doping level. The salt solution was then quickly replaced with a precise volume of deionized water at t = 0 s and the conductivity of the solution was measured every ten s using a four-probe conductivity cell (Orion 013005MD, Thermo Scientific) and a conductivity meter (Orion 3 star, Thermo Scientific) until a conductivity plateau was reached (see Supporting Information Figure S4). The temperature was maintained at 25.0 ± 0.1 °C using a water jacket connected to a temperature controlled water circulator (ThermoHaake K20). The PEC was then dried at 120 °C for 12 h and the mass of the dry PEC was recorded. A similar procedure was used to study ion diffusion as a function of temperature. The same PEC doped in 0.1 M NaCl was used throughout the experiment and the solution conductivities were recorded as a function of time at five temperatures (5, 15, 25, 35, 45 °C). Standard solutions of NaCl were used to convert conductivity into concentration. Each standard was measured at the temperature of the ion release experiment.

Radiolabeling Studies The excess of PMAPTAC or PMANa within pair **B** was measured (to a greater precision and accuracy than possible with NMR) using radiolabeled counterions $^{35}SO_4^{2-}$ (^{35}S , half-life 87.4 d, β emitter, E_{max} = 167 keV, supplied with a specific activity of 750 Ci mol⁻¹) and $^{22}Na^+$ (half-life 950 days, positron, γ emitter, E_{max} = 546 keV, produced with a specific activity of 914.66 Ci g^{-1}) using a procedure described in detail recently. 36

Small Angle Neutron Scattering (SANS). Deuterated PMA (n = 4010) was neutralized with NaOH. Two different PMANa complexes with PMAPTAC (n = 3850) were prepared for SANS:

one for background measurements was prepared using 100% H-PMANa (n = 3600) whereas that used for the sample was a mixture of 20% D-PMANa and 80% H-PMANa.

To achieve matching of the neutron scattering length densities (SLDs) of non-deuterated PMANa ("contrast matching"),³⁷ the atomic composition of the non-deuterated complex, expressed as $C_{14}H_{26}N_2O_3(H_2O)_x(D_2O)_yNaCl$, was obtained from the molar ratios of the components at various $H_2O:D_2O$ volume ratios, then the SLDs were calculated with the NIST online calculator (density = 1.1 g cm⁻³, sample thickness = 1 mm, and neutron wavelength, λ = 6Å). The SLD of the background solvent, $(H_2O)_x(D_2O)_yNaCl$, was calculated at different $H_2O:D_2O$ volumetric ratios. A match was found at 25.5% D_2O thus PECs were immersed in 0.1 M NaCl in 25:75 $D_2O:H_2O$.

After the PECs were separated from the dilute phase, the initial NaCl solution in H₂O was replaced with 20 mL NaCl (0.2 M) in 25:75 by volume D₂O:H₂O. This solution was replaced with a fresh one after 24 h. The mixture was then annealed for 24 h at 60 °C then allowed to cool to room temperature at a rate of 5° C h⁻¹ to allow the polymer chains to attain an equilibrium conformation. The samples were transferred into quartz cuvettes (1 mm path length, VWR). Neutron diffraction was performed at room temp at the Oak Ridge National Laboratory on beamline 6 (EQ-SANS) with a coupled supercritical hydrogen moderator. The source-to-sample distance was 14 m while the sample-to-detector distance was varied between 1 m and 9 m to obtain a range of scattering vector Q (= $\frac{4\pi}{\lambda} sin\theta$) values between 0.003 and 0.06 Å⁻¹. The dimensions of the detector were 1 m x 1 m with a resolution of 5.5 x 4.3 mm. The non-deuterated background was normalized then subtracted from the deuterated sample. After normalization, the program SasView was used to fit the data to the expected scattering intensity versus Q for a monodisperse Gaussian coil.

Isothermal Titration Calorimetry. PMAPTAC, PMANa, and NaCl were dried for 4 h at 120° C. 8.10 mM PMANa solutions adjusted to pH 11.5 with NaOH to ensure complete ionization in 0.050

M NaCl were titrated into 1.4545 mL 0.5 mM PMAPTAC (also pH 11.5 in 0.05 M NaCl) using a VP-ITC (MicroCal Inc.) calorimeter. Complexation was endothermic (see Supporting Information Figure S5) with a Δ H of complexation of about 4 kJ mol⁻¹.

Results and Discussion

The rest of this report is laid out as follows: first, the individual polyelectrolytes and their characterization are discussed. After verifying the stoichiometry of Pol+:Pol- made from these polyelectrolytes was near 1:1, PECs were doped to equilibrium with NaCl at various concentrations. The composition (mole fraction polymer, salt, water) of each PEC was again measured. The equilibrium coil size of one of the PECs was determined with neutron scattering to provide a reliable method of translating experimental degrees of polymerization to the number of (theoretical or normalized) Kuhn repeat units representing a Gaussian chain. The diffusion of ions within PECs was then modeled and measured by allowing NaCl to diffuse out of materials. Since counterion dynamics are assumed to reflect polymer dynamics, ion diffusion coefficients were translated to ion hopping frequencies, which were inverted to provide ion hopping times and equated to polymer repeat unit relaxation times. Linear viscoelastic responses for undoped PECs made from five matching Pol⁺Pol⁻ pairs were determined using rheology. Time-temperature superposition provided key relaxation times and the rubber plateau modulus for these wellentangled systems. Finally, these relaxation times were considered in the context of "sticky interactions" and a relationship between zero shear viscosity and chain length was derived and tested against the data.

Fractionation of broad molecular weight PMAPTAC and PMANa prepared by polymerization in water yielded several samples of narrow polydispersity material with molecular

weights greater than 10⁵ g mol⁻¹ (see Table 1 and Figures S1 and S2, Supporting Information). The polydispersities were significantly lower than those obtained previously using aqueous RAFT polymerization.³⁶ From these fractions, five PMAPTAC/PMANa pairs were selected with matching degrees of polymerization, n_{avg}, covering average n values of 1070 to 4740 (Table 1), well above the entanglement n of 343 found in our previous work on the same system.³⁶ The spacing between each monomer repeat unit was two backbone carbons or 0.252 nm. The compositions of PECs prepared from these pairs were carefully determined by dissolving them in 1.0 M KBr in D₂O and integrating the relevant NMR bands (Supporting Information Figure S3). The deviation from 1:1 charge stoichiometry was 4% or less (Table 1).

PEC Composition

Once they are formed, the equilibrium composition of PECs is under the reversible thermodynamic control of the salt concentration of solutions in which they are immersed. Salt reversibly "dopes" the PEC according to Equation 2 and the water content also adjusts accordingly. The salt contents of PEC made with the broad $D_{average} \approx 1.4$ starting materials (see Figures S1 and S2 in Supporting Information) immersed in various [NaCl] were determined by releasing the ions into pure water (Supporting Information Figure S4), measuring the conductivity, then drying the salt-free samples to determine water and polyelectrolyte weight%. The compositions are summarized in Table 2. A molecular weight dependence on the stability of PECs to high salt concentration has been observed. 18, 38 At lower salt concentrations, such as those used here, Li et al. report little composition dependence for PECs made from polypeptides above a degree of polymerization of 50.18 PECs similar to those used here made with 150 versus 510 repeat units showed less than 10% difference in composition at high polymer volume fractions. 38 The independence of composition on molecular weight beyond similar n values was predicted by Qin et al. 39

Table 2. Compositions and Ion Dynamics of PEC as a Function of Salt Concentration at 25 °C.

Salt Concentration ^a	0.01 M	0.05 M	0.1 M	0.15 M	0.2 M
wt% PEC	25.0	21.9	20	18.7	17.4
wt% water	74.9	77.9	79.4	80.3	81.4
wt% NaCl	0.11	0.25	0.61	0.95	1.17
ф РЕС ^b	0.23	0.2	0.19	0.17	0.16
ф _{water}	0.77	0.79	0.81	0.82	0.83
φ _{NaCl} x 10 ⁻³	0.53	1.20	2.87	4.48	5.55
°[NaCl] _{PEC,} M	0.02	0.05	0.11	0.17	0.22
^d y	0.02	0.06	0.15	0.25	0.33
$^{e}D_{i,PEC} \times 10^{7} cm^{2} s^{-1}$	0.91	1.15	2.20	3.00	3.50
d (nm) ^f	0.96	1.00	1.03	1.05	1.08
$ au_{ m hop} = au_{ m p} \; (m ns)^{ m g}$	16.9	14.5	8.04	6.13	5.55
^h p x 10 ⁴	2.00	2.33	4.20	5.51	6.09

ⁱE_{open} x10⁻⁴ kJ mol⁻¹ 2.11 2.07 1.93 1.86 1.83

^asolution salt concentration: [NaCl]_s

 $^{b}\Phi_{PEC}$ = volume fraction PEC

^cPEC salt concentration

doping level

^ePEC ion diffusion coefficient

fdistance between Pol+Pol- pairs

gion hopping relaxation time = Pol⁺Pol⁻ monomer relaxation time

hhopping probability

ⁱE_{open} = -RTInp

density of PEC was 1.1 g cm⁻³

The doping level, y, is presented as the mole ratio of NaCl to PMAPTA/PMA (PMAPTAC and PMANa lose their counterions when they complex). It is assumed that every NaCl introduced breaks one Pol+Pol- pair and all the ions become counterions for polyelectrolyte repeat units, as implied by Equation 2. For example, if y = 0.1 then 10% of the Pol+Pol- "intrinsically compensated" pairs have been converted to Pol+Cl- and Pol-Na+ "extrinsic" counterion-compensated units.⁴⁰ In previous work on PDADMA/PSS PECs it was shown that this assumption was valid up to about y = 0.2, after which some of the salt entering the PEC is believed to exist as co-ions (using terminology from the ion-exchange literature⁴¹). The doping level varies linearly with [NaCl] over the range 0 to 0.2 M NaCl (Figure 1) according to $y = K_{unpair}[NaCl]$ where K_{unpair} is a constant that

depends on the identity of salt MA along a Hofmeister series. K_{unpair}, the inverse of an association or pairing constant, K_{pair}, also depends on the polyelectrolyte repeat units Pol⁺ and Pol⁻. More compact pairs of Pol⁺Pol⁻ having fewer waters of hydration yield PECs that are more resistant to salt doping (K_{unpair} is smaller).³³

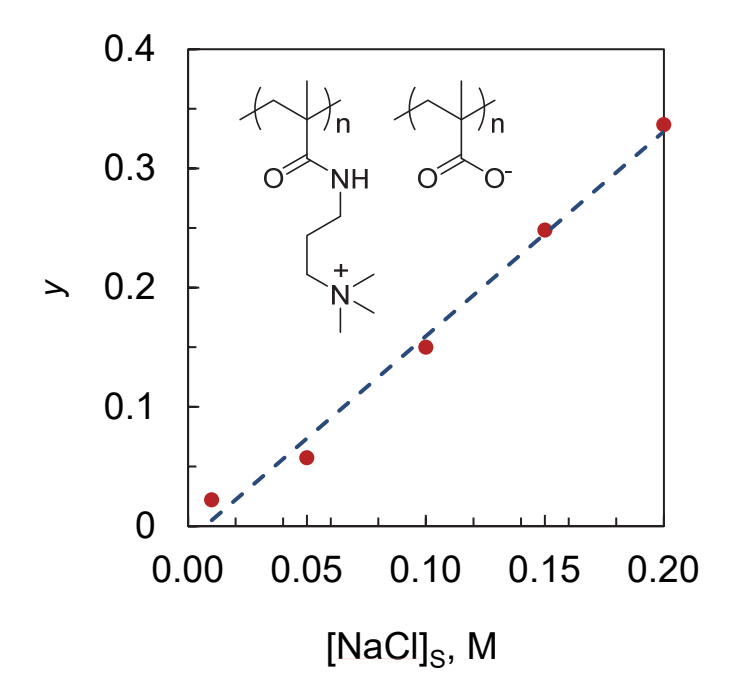


Figure 1. Dependence of the doping level *y*, which is the fraction of PMAPTA/PMA pairs broken by NaCl, *versus* the solution concentration of NaCl for a stoichiometric PMAPTA/PMA PEC at 25 °C. Dotted line: *y* = 0.01 + 1.69[NaCl]. Inset shows structures of PMAPTA (left) and PMA (right). *Coil Size from Small Angle Neutron Scattering (SANS)*

In order to compare the experimental results with theory the length of the chain must be represented by N Kuhn segments, each of length b, representing a freely jointed chain having Gaussian statistics. The Kuhn length may be determined from the size (R_g) of the polymer coil, $b = 6R_g^2/nl$ where n is the number of monomer repeat units of length l (0.252 nm) and Nb = nl.

SANS, previously employed for structural information on protein/polyelectrolyte complexes, ^{21, 37, 42, 43, 44, 45} and synthetic polyelectrolyte PECs, ^{21, 46, 47} was used for a direct measurement of the coil size of deuterated PMA dispersed in a PEC. D-PMANa (n = 4010) was diluted with protiated PMANa (n = 3600) in a 1:4 ratio (20% D-PMA) to separate interchain from intrachain correlations. ^{21, 37, 43, 46} The H/D-PMANa mixture was complexed with PMAPTAC (n = 3850). All non-deuterated components were then contrast matched with a mixture of D₂O and H₂O. A nondeuterated PEC sample was used for background subtraction under the same conditions.

Figure 2 shows mainly the (Guinier) region of scattering which is assumed to correspond to the random coil shape factor of D-PMA coils within the PEC.

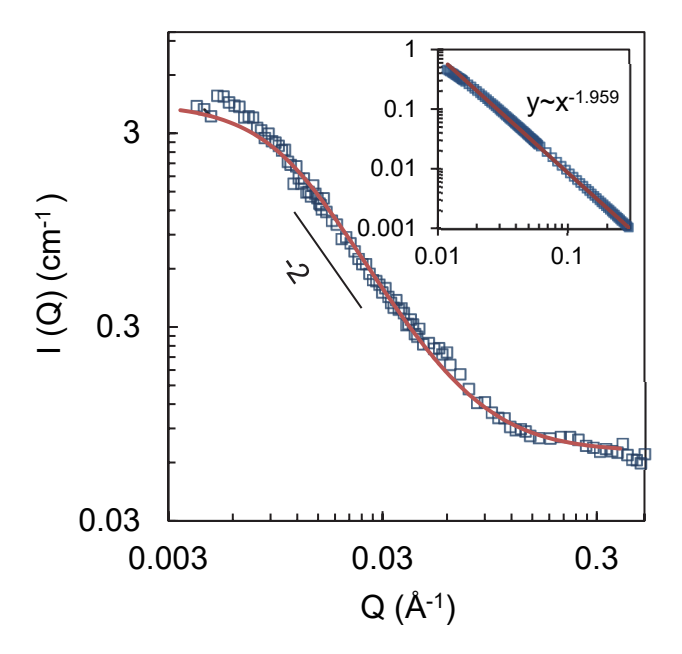


Figure 2. Small-angle neutron scattering profiles for PMAPTA/PMA polyelectrolyte PEC with D-PMA of 4010 repeat units diluted with H-PMA, n = 3600, in PMAPTA n = 3850 doped in 0.1 M NaCl at 25 $^{\circ}$ C. Squares are the data after background normalization and subtraction, and the line is the fit (χ^2 of 5.4) obtained by the Debye function for a Gaussian polymer with R_g = 15.7 nm. The scattering intensity in the Guinier region decays as Q-1.959.

The fit for a random-coil model shows a radius of gyration R_g of 15.7 \pm 0.4 nm, yielding a Kuhn length of 1.5 nm. Fits to R_g of 13.7 nm and 17.7 nm in Supporting Information Figure S6 are intended to support the stated accuracy of this measurement. The inset in Figure 2 shows a scaling of -1.959, very close to the expected -2.0 for a coil with Gaussian statistics. These findings may be compared with the few SANS measurements of coil sizes of synthetic polyelectrolytes within PECs. For example, our group measured R_g of deuterated PSS in a PDADMA/PSS complex^{46, 47} and Spruijt et al. determined R_g for a PEC of similar composition to that used here - poly(N,N-dimethylaminoethyl methacrylate) with sodium polyacrylate.²¹ D-PSS within PDADMA/PSS was rather tightly coiled, not too far expanded from protiated PSS in a θ -solvent.⁴⁶ In contrast, Spruijt reported a wide range of Kuhn lengths, 3.5 to 16 nm, corresponding to more expanded complexes.²¹ They also noted that these lengths were probably upper limits, so we used a Kuhn length of 3 nm (twice the actual value) in prior studies of the viscoelasticity of PMAPTA/PMA PECs.³⁶

The finding that the coil was nearly Gaussian is important for comparison to theory, especially to properties related to molecular weight: if the coil is random, R_g scales as $N^{1/2}$.⁴⁸ Also, in a previous study in PSS/PDADMA PECs we found the coil size to be surprisingly independent of salt concentration over the range 0.1 - 1.2 M KBr.⁴⁷ Thus, it is believed that the PMA coil size (Kuhn length) does not change significantly with [NaCl]. Table 1 lists the average N values for the five pairs of polyelectrolytes used to make PECs.

Counterion Dynamics

PEC composition measurements also provided the opportunity to determine diffusion coefficients of NaCl in PECs under various conditions. The conductivity of well-stirred solutions above PECs made from $\Theta_{average} \approx 1.4$ PMAPTAC and PMANa doped to different [NaCl] was converted to concentration with the aid of conductivity standards and fit as a function of time to

the equation describing diffusion of species out of one side of a plate geometry (finite boundary conditions)⁴⁹

$$\alpha = \frac{M_t}{M_{\infty}} = 1 - \sum_{m=0}^{\infty} \frac{8}{(2m+1)^2} \exp\left(\frac{-D_{i,PEC}(2m+1)^2 \pi^2 t}{4\sigma^2}\right)$$
 [3]

where α is the fraction of NaCl that has diffused out of the PEC at time t, M_t is the mass diffusing out at t, M_{∞} is the mass diffusing out at infinite time, $D_{i,PEC}$ is the average uniform diffusion coefficient of Na⁺ and Cl⁻ within the PEC, assumed to remain constant for a specific [NaCl] and temperature, σ is the thickness of the PEC film at the bottom of the vial (typically about 0.02 cm and m is an integer 0,1,2,3... At α less than 0.7 the approximation for semiinfinite diffusion holds well.⁴¹

$$\alpha = \frac{2}{\sigma} \sqrt{\frac{D_{i,PEC}t}{\pi}}$$
 [4]

 α is plotted as a function of $t^{1/2}$ in Figure 3.

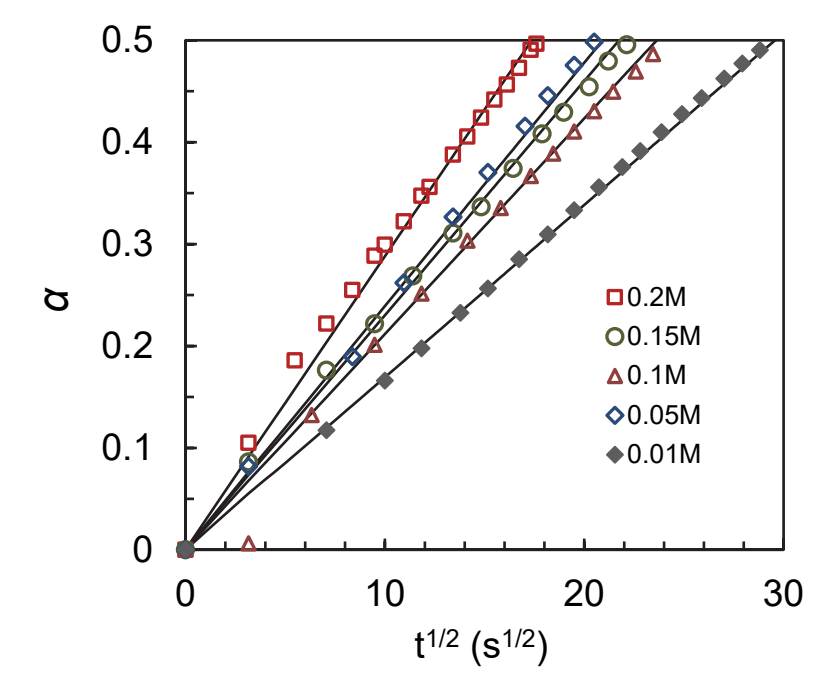
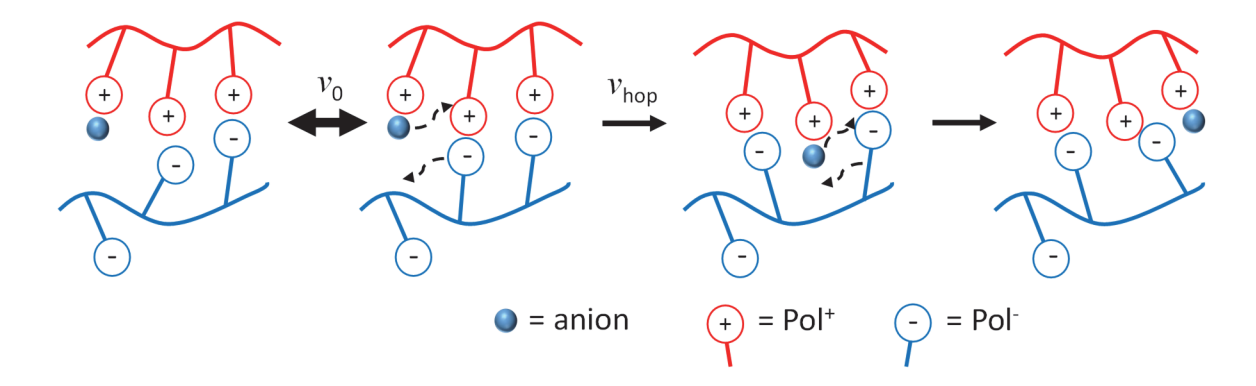


Figure 3. Fraction α of NaCl diffusing out of PECs made from $\mathfrak{D}_{average} \approx 1.4$ PMAPTAC and PMANa doped to different levels *versus* t^{1/2}. Solid lines are fits to finite diffusion from a plate (planar geometry), Equation 3 using the NaCl diffusion coefficient within the PEC, $D_{i,PEC}$, as the only fit parameter.

Diffusion data for ions in PECs provides a profile of counterion dynamics. The microscopic picture of ion transport in ion-containing polymers usually invokes ion jumps or hops between sites. Under the simplest view, hopping occurs among nearest neighbor sites of distance *d* from each other⁵⁰

$$D_{i,PEC} = \frac{d^2}{6\tau_{hop}} = \frac{\nu_T d^2}{6}$$
 [5]

where τ_{hop} is the ion hopping relaxation time and ν_T the hopping frequency at temperature T. Unlike many ion containing polymers,⁵¹ PECs show no evidence for clustering of ions⁵² and no other evidence for nonuniform distributions of components, unless they have been prepared by the multilayering method, in which case they exhibit some degree of "fuzzy" stratification.⁵³ The density of hopping sites is thus the density of Pol⁺ or Pol⁻ repeat units, which is estimated from the bulk density of the PEC and the molecular weights of components. Estimates for *d* are given in Table 2. The hopping rates for various doping levels *y*, calculated from Equation 5, also listed in Table 2, indicate hopping frequencies increasing slightly with added salt from 5.7 x 10⁷ to 1.8 x 10⁸ s⁻¹. Despite slight increases in the hopping distance, hopping rates increase, probably because of a decrease in the activation energy from the plasticizing effect of additional water in the PEC when it is doped (Supporting Information Figure S7).



Scheme 1. Illustrating hopping of ions from site to site. Each hop is coupled to and controlled by the dynamics of the polyelectrolyte repeat unit with which the ion is associated. A hop occurs when an intrinsic Pol+Pol- pair exchanges with an extrinsic Pol+A- pair (in this example). Most of the Pol+Pol- breaking attempts, occurring with frequency v_0 , simply reform the same pair.

Variable temperature measurements of $D_{i,PEC}$ using PEC doped in 0.1M NaCl (y = 0.17) show the diffusion to be thermally activated i.e

$$D_{i,PEC} = D_0 e^{\frac{-E_a}{RT}}$$
 [6]

where D_0 , the preexponential factor, from the intercept in Figure 4, is 5.51 x 10⁻⁴ cm² s⁻¹

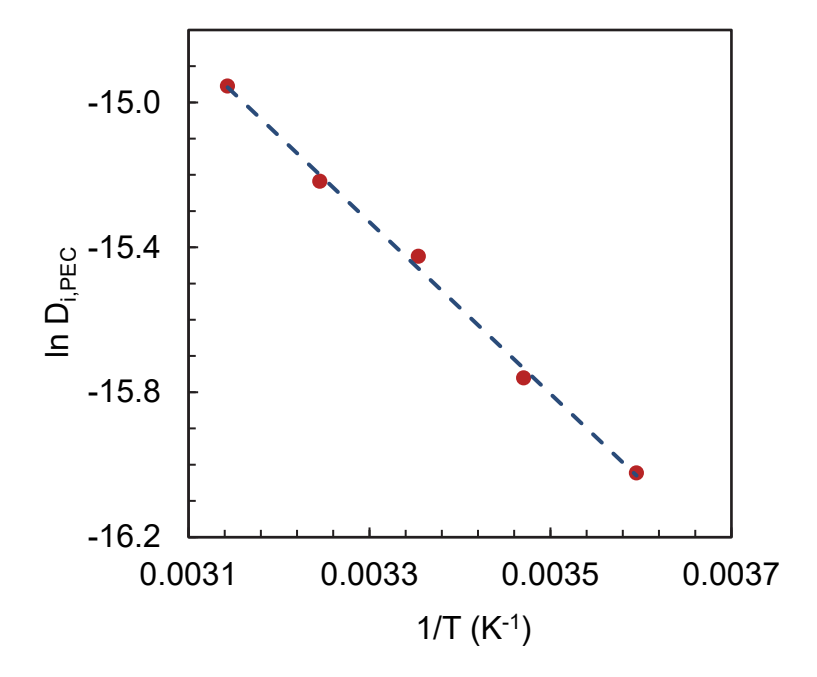


Figure 4. Arrhenius plot of the log of the diffusion coefficient (in cm² s⁻¹) versus 1/temperature for ion transport in PEC made from $\Theta_{average} \approx 1.4$ PMAPTAC and PMANa doped with 0.1 M NaCl. The slope provides an activation energy of 19.7 kJ mol⁻¹.

The activation energy, E_a, for hopping from Figure 4 is 19.7 kJ mol⁻¹. Assuming *d* in Eq. 5 does not change with temperature

$$v_T = v_0 e^{-\frac{E_a}{RT}} \tag{7}$$

Where v_0 is interpreted to be a hopping attempt frequency, here 3.12 x 10¹¹ s⁻¹ (3.2 ps, from Eq. 5 when $D_{i,PEC} = D_0$) Equation 7 can also be understood by

$$v_T = v_0 p \tag{8}$$

where p is the probability a hopping attempt is successful. Alternatively, p can be considered the fraction of Pol^+Pol^- open at any instant in time and the fraction closed ≈ 1 . A value of $p = 2.0 \times 10^{-4}$ gives an energy difference = -RTln[open/closed] = -RTlnp of 21.1 kJ mol⁻¹ at room temp, (kT at

room temp = 2.48 kJ mol⁻¹), and also close to the activation energy from Figure 4. With the idea that $E_{act} = E_{open}$, Table 2 lists E_{open} for the other [NaCl] studied.

Polymer Dynamics

As with most studies of ion transport in ion-containing polymers, counterion dynamics are believed to be coupled to polymer dynamics.³⁴ The cartoon in Scheme 1 suggests motions in polyelectrolyte pendant groups accompany an ion hop. Not shown are any rearrangements of the water molecules hydrating each charge pair. Undoped PECs represent an unusual form of charged polymers: they are polyelectrolytes without counterions. When hydrated, they are also viscoelastic materials with exceedingly high viscosities.^{20, 24, 26, 54, 55, 56} Dynamics of polymers may be probed using rheological methods. In the present case, a laboratory rheometer operating over the frequency range 0.01 to 100 s⁻¹ was used to determine storage and loss moduli, as well as viscosity for PECs immersed in salt solutions.

To expand the effective range of frequency measurements, viscoelastic measurements were made at different temperatures and the data at each temperature were shifted along the frequency axis by a shift factor a_T and along the modulus axis by a factor b_T to yield time-temperature superposition.⁴⁸ Typical results are shown in Figure 5, which also highlights three important frequencies (or the inverse, relaxation times) for entangled polymers (PECs with other pairs are shown in Supporting Information Figures S8 and S9): the lowest frequency corresponds to the time, τ_{rep} , it takes a polymer chain to wriggle, or reptate, out of a tube it has made for itself.⁴⁸ This is followed, at higher frequencies by a pseudo-plateau region in the modulus which is a result of entanglements that act like dynamic crosslinks.⁴⁸ At higher frequencies is a crossover corresponding to the entanglement time, τ_e , which is the relaxation time of the parts of the polymer

chains caught between entanglement points. At the highest frequency measured there is another relaxation, τ_q which we have attributed to exchanges between neighboring pairs of Pol⁺Pol⁻.³⁶

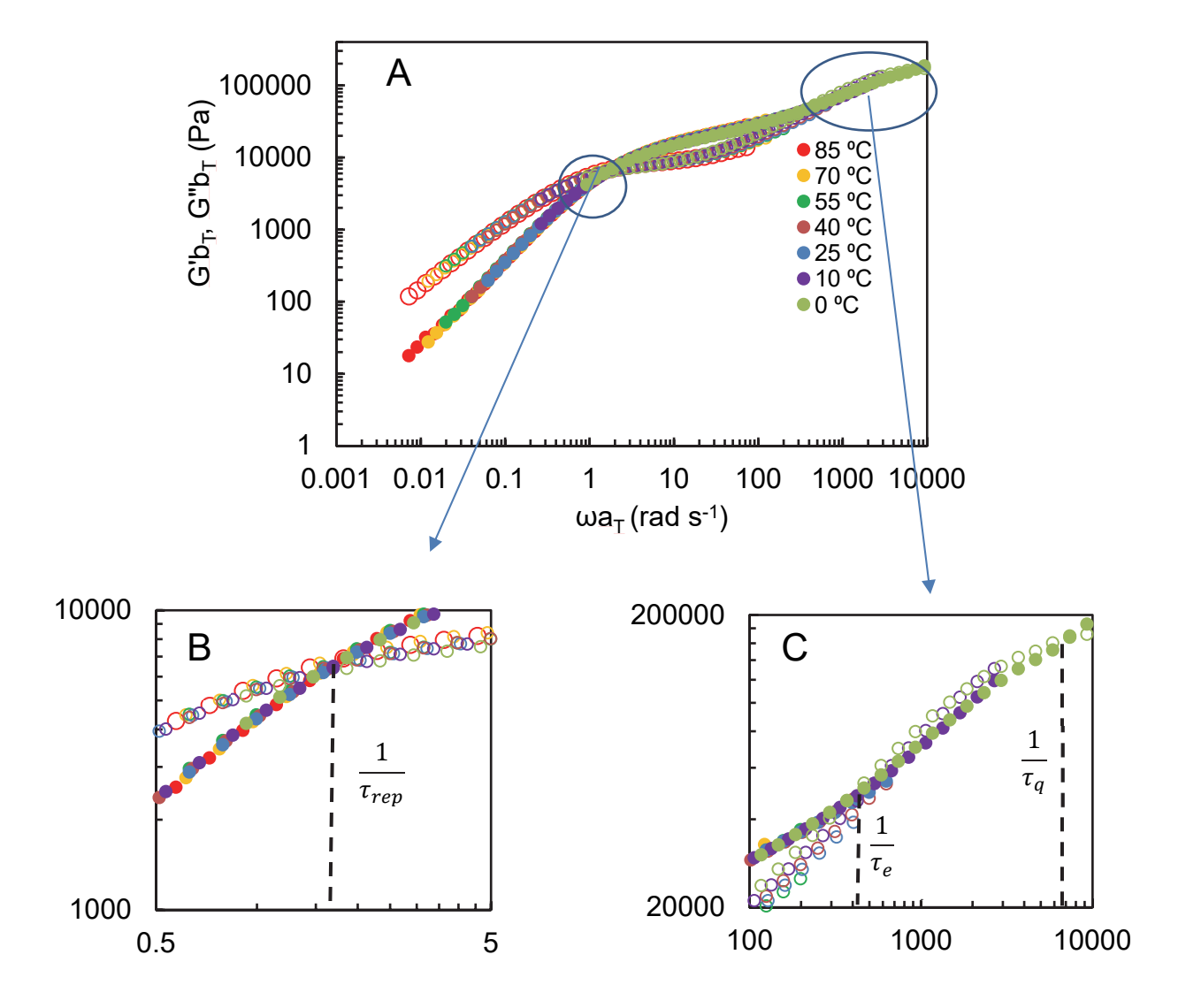


Figure 5. Storage modulus G' (filled circles) and loss modulus G" (open circles) for PEC Pair **E** (n_{avg} = 1070) in 0.01 M NaCl as a function of frequency. Reference temperature 25 °C. Time-temperature superposition has been used to stitch together data recorded at different temperatures (shown in Panel A) using the shift factors a_T and b_T in Supporting Information Figure S10. Zoom-in panels B and C highlight three intersections of G' and G" which show relaxation times (= 1/frequency) of significant interest: reptation time τ_{rep} at about 0.55 s, entanglement time τ_e at about 1.96 x 10⁻³ s and a time τ_q at about 1.35 x 10⁻⁴ s, believed to represent the pair exchange time of neighboring Pol+Pol- pairs.

Exposing complexes to pure water was avoided. We and others have found that PECs may gradually inflate because they exert osmotic pressure relative to pure water. This behavior leads to a sharp upturn in water content and the appearance of pores (leading to opacity) within the PEC as $[NaCl] \rightarrow 0.57$ Thus, the minimum salt concentration used was 0.01 M NaCl, which yielded a small level of doping (about 2%) but is assumed to represent *substantially undoped* PEC. The viscoelastic behaviors of all the (nearly) undoped pairs of PECs are shown in Figure 6. With increasing molecular weight, the rubbery plateau becomes more apparent.

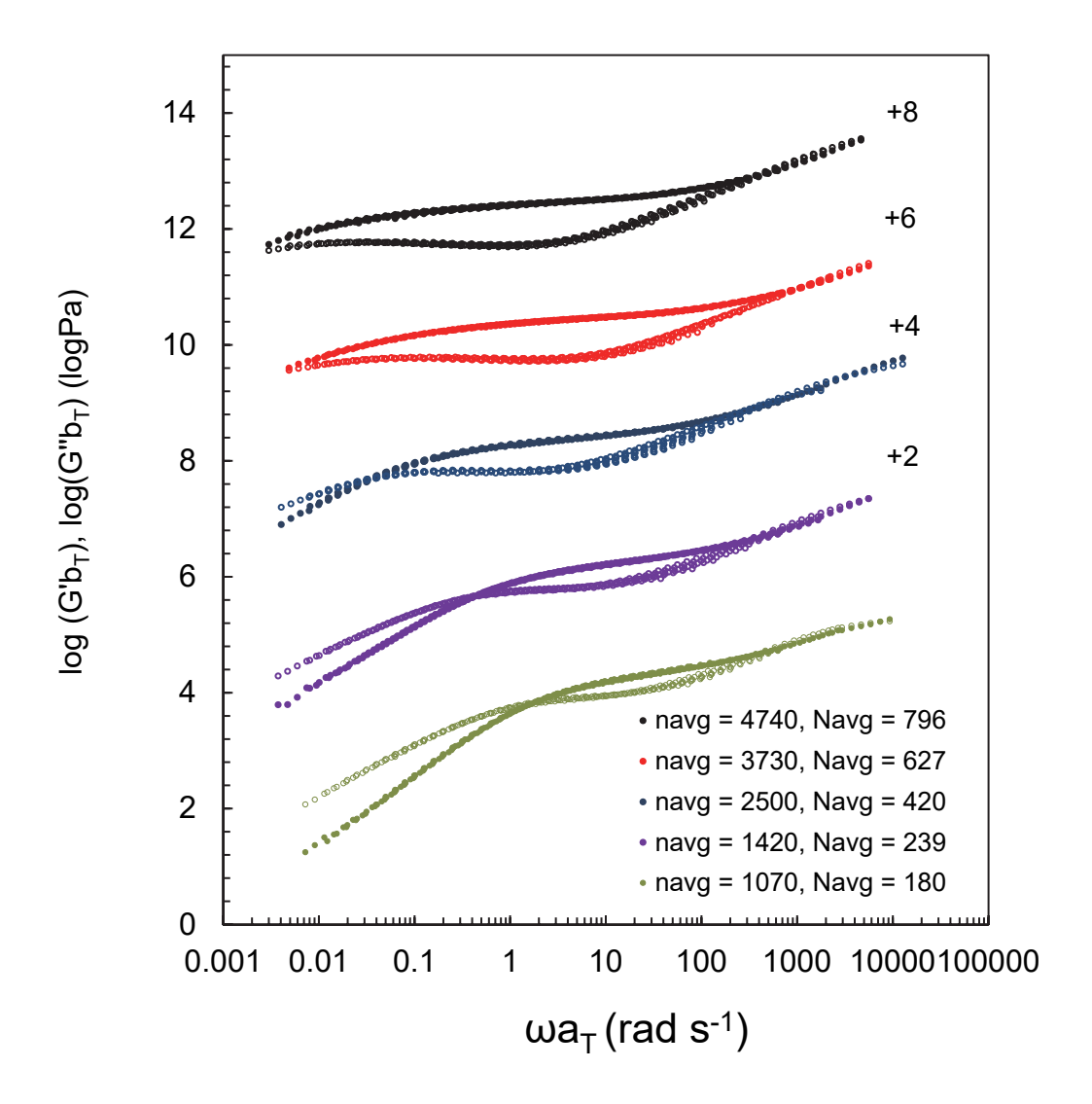


Figure 6. Viscoelastic response, G' closed symbols, G" open symbols, using time temperature superposition of the data in Figure S8, of five pairs of PMAPTA/PMA PECs having increasing (average) molecular weights, represented by the number of repeat units n_{avg} or N_{avg} shown. Each curve except n_{avg} = 1070 has been shifted upwards by the indicated number of log frequency units (2, 4, 6, or 8). The frequency range of the rubbery plateau grows as $1/\tau_{rep}$ shifts to lower frequencies, although the plateau modulus, G_0 , remains constant. Reference temperature = 25 °C. Both τ_e and τ_q show no dependence on molecular weight.

In classical polymer rheology, some parameters are expected to change and others are not. Table 3 summarizes the key points from Figure 6. First, the value of the storage modulus at the rubbery plateau, G_0 , is independent of molecular weight (indicated by the number of repeat units, n_{avg}), as expected.⁴⁸ Also expected is the finding that τ_e and τ_q are (approximately) constant as a function of chain length.

Table 3. Relaxation times, plateau modulus and viscosity of PECs having various molecular weights. All values given at a reference temperature of 25 °C.

Pair (N _{avg})	A (796)	B (627)	C (420)	D (239)	E (180)
G _o (kPa)	17.6	26.3	22.1	16.3	18.9
τ_{rep} (s)	1400	200	25	2.5	0.55
^a τ _{rep,calc} (s)	1500	450	62	3.7	0.89
τ _e x 10 ⁻³ (s)	2.71	1.32	2.80	2.82	1.96
$\tau_q \ x \ 10^{-4} (s)$	1.65	1.13	1.98	1.78	1.35
⁵η₀ (Pa s)	-	-	8.9 x 10 ⁵	5.5 x 10 ⁴	1.6 x 10 ⁴
η₀ from G₀τ _{rep} (Pa s)	2.45 x 10 ⁷	5.97 x 10 ⁶	5.53 x 10 ⁵	4.08 x 10 ⁴	1.04 x 10 ⁴
^c η _{o, calc} (Pa s)	2.75 x 10 ⁷	8.34 x 10 ⁶	1.13 x 10 ⁶	6.71 x 10 ⁴	1.63 x 10 ⁴

^acalculated from Equation 17

^bdirect experimental

^ccalculated from Equation 18

activation energies, determined according to the Arrhenius relationship,

$$ln\left(\frac{a_T}{a_{T,ref}}\right) = \frac{E_a}{R} \left(\frac{1}{T} - \frac{1}{T_{ref}}\right)$$
 [9]

using a T_{ref} of 25 °C are plotted in Supporting Information Figure S11 and show an average E_a = 44.3 kJ.

Semenov and Rubinstein provided a theory of the viscoelastic response of unentangled and entangled polymers having "sticky" interaction points.⁵⁸ In comparison with neutral polymers

having no sticky interaction points, such as Pol⁺Pol⁻ pairs, characteristic times in Figures 5 and 6 and Table 3 are strongly shifted towards lower frequencies.

Modulus G_0 (determined experimentally by the value for G' at the point where $tan\delta$ (= G''/G') is a minimum) is expected to be given by⁴⁸

$$G_0 = \left(\frac{kT}{d^3 N_e}\right) \phi_{PEC}$$
 [10]

Where $1/d^3$ is the chain density and ϕ_{PEC} the volume fraction of polymer (d and ϕ_{PEC} listed in Table 2). N_e is the number of repeat units between entanglements, estimated using data from our prior work on the same system,³⁶ which found n_e = 343 therefore N_e = 58. Using d = 0.96 nm, G₀ for PEC in 0.01 M NaCl was calculated to be 18 kPa, similar to the average of the experimental G₀ values in Table 3.

The viscosity (at zero shear) η_0 is another parameter of interest. Because the viscosities were so high, only the PECs with the three lowest n_{avg} values could be measured at zero shear. The rest of the viscosities were estimated from the relationship^{48, 58}

$$\eta_0 \approx G_0 \tau_{ren} \tag{11}$$

The three measured viscosities (Supporting Information Figure S9) showed good agreement with those determined using Equation 11

A plot of the viscosity of undoped PECs versus the chain length (Figure 7) revealed a completely unexpected behavior: η_0 scales with n⁵ whereas the classic result for entangled nonsticky polymers is $\eta_0 \sim n^3$ in theory⁴⁸ (and $\eta_0 \sim n^{3.4}$ experimentally⁵⁹). We previously adapted Rubinstein and Semenov's sticky reptation theory to interacting polyelectrolytes to yield a scaling of $\eta_0 \sim n^3$ which appeared to be supported by the two closely-spaced data points we had for PECs

with chain lengths not far above n_e .³⁶ This prior data may still have been in the viscosity transition regime just above n_e .

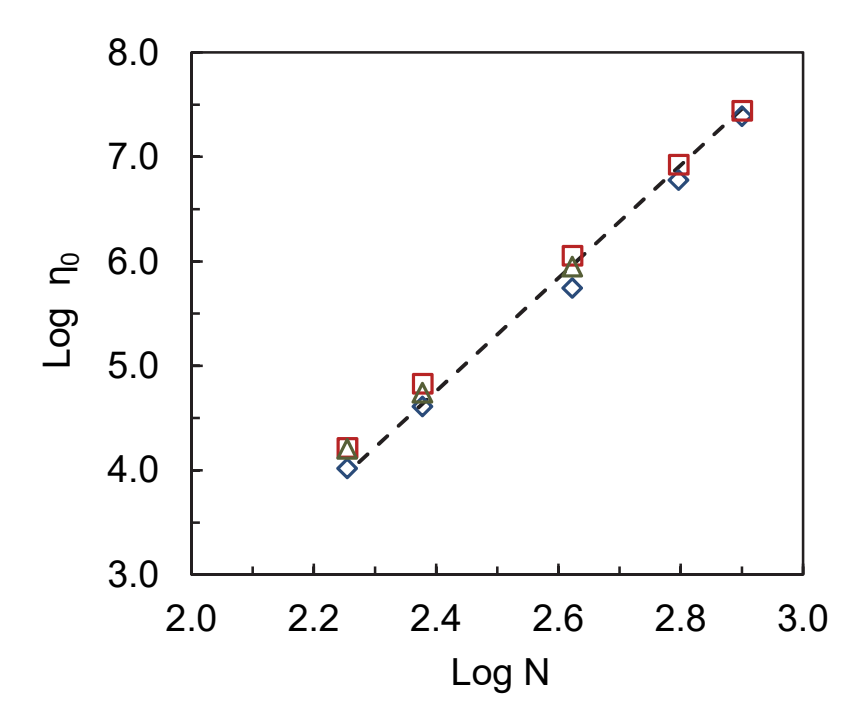


Figure 7. Log-log plot of zero shear viscosity η_0 , in Pa s, at 25 °C versus number of Kuhn repeat units to show the scaling behavior. Δ, η_0 directly measured experimental; \Diamond , experimental η_0 from measured $G_0\tau_{rep}$; \Box , calculated η_0 using Equation 18. The dotted line illustrates a scaling of $\eta_0 \sim N^{5.4}$ whereas the expected theoretical scaling for nonsticky entangled polymers is $\eta_0 \sim N^3$ (using the simplest level of theory) and the experimental scaling is $\eta_0 \sim N^{3.4}$ (also predicted by more advanced theory⁶⁰).

Relaxation Times

The plateau modulus estimated from Equation 11 is in agreement with that measured, which means the enhanced viscosity is attributed to a much longer τ_{rep} than would be observed for a nonsticky system that is equivalent in all other respects. Since the characteristic relaxation times

discussed above are quantitative signposts to understanding polymer dynamics,⁴⁸ they are presented here, along with their significance, in order fastest to slowest:

 τ_{p}

The fastest relaxation time is typically called the "monomer relaxation time," τ_p , which controls all the other slower dynamics. Typically on the time scale of 10^{-9} s, it may be observed with dielectric spectroscopy. In the present case it is assumed to be the same as the ion hopping time in Scheme 1.

$$\tau_{hop} = \tau_p = \tau_0/p \tag{12}$$

In other words, τ_p is the time between Pol⁺Pol⁻ unpairing events shown in Scheme 1. In this assumption, the ion hopping is coupled to and controlled by the dynamics of the polyelectrolyte segments. In a previous work it was assumed that the dynamics of Pol⁺Pol⁻ opening was first order with respect to the salt concentration within the PEC,³⁶ i.e. the rate of A⁻ hopping from monomer Pol₂⁺ to monomer Pol₁⁺ and replacing Pol⁻, represented by extrinsic/intrinsic pair exchange

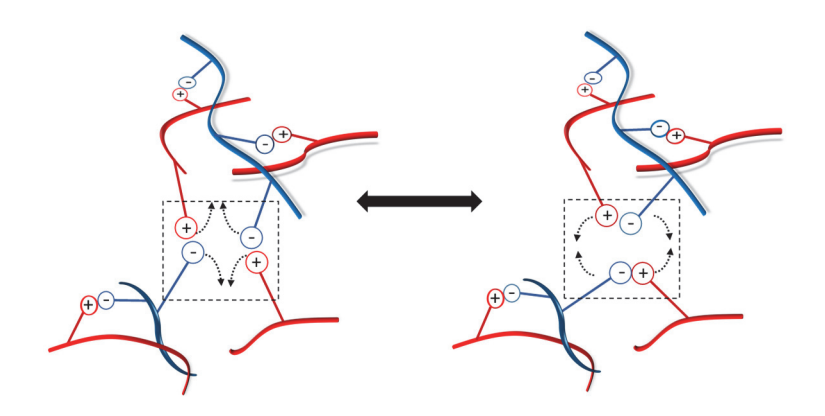
$$Pol_{1}^{+}Pol^{-} + Pol_{2}^{+}A^{-} \rightarrow Pol_{1}^{+}A^{-} + Pol_{2}^{+}Pol^{-}$$

depends on $[Pol_2^+A^-]$. If this were true, a plot of the rate versus $[Pol_2^+A^-]$ should be linear, but it is not (Supporting Information Figure S12). The hopping rate does not change much with [NaCl] (zero order in [NaCl]) and the small acceleration is due to a small decrease in E_a with increasing doping (Figure S7, Supporting Information). The attempt frequency v_0 for hopping/pair breaking is much faster, but only a small fraction p of these attempts leads to an extrinsic/intrinsic pair exchange.

In order for net segmental displacement (allowing the entire molecule to diffuse), a pair of Pol⁺Polunits needs to exchange. τ_q is the time between quad (correlated pair) breaking events, illustrated in Scheme 2, which is τ_p /the probability that the broken pair will find an open bond next to it.

$$\tau_a = 2\tau_p (1 - y)/p \tag{13}$$

The factor of 2 accounts for the fact that half of the time the two neighboring pairs will re-pair with their original partners and the other half of the time they will switch places. For the undoped series in Table 3, $\tau_p = \tau_{hop} = 16.9$ ns and $p = 2.0 \times 10^{-4}$, which yields $\tau_q = 1.7 \times 10^{-4}$ s, close to the average τ_q of 1.6×10^{-4} s in Table 3.



Scheme 2. Illustration of the Pol⁺Pol⁻ pair exchange mechanism for allowing neighboring segments of polymer to temporarily detach from each other and for chains to exhibit net motion relative to each other. This is a Pol⁺Pol⁻/Pol⁺Pol⁻ intrinsic pair rearrangement (4 pendant groups or a "quadrupole") in contrast to the ion hopping in Scheme 1 which is an extrinsic/intrinsic pair exchange.

 τ_{e}

For nonsticky polymers, theory gives⁴⁸

$$\tau_e \approx \tau_p N_e^2. \tag{14}$$

For f_e stickers between entanglements, if f_e >1, the entanglement relaxation time will be slowed by a factor f_e

$$\tau_e \approx \tau_p f_e N_e^2 \approx \tau_p (1 - y) N_e^3$$
 [15]

since $f_e = (1 - y)N_e$. τ_e calculated using Equation 15 (y = 0.02, $\tau_p = 1.67$ x 10^{-8} s, $N_e = 58$) is 2.6 x 10^{-3} s, compared to the average experimental $\tau_e = (2.3 \pm 0.6)$ x 10^{-3} s of the various N's in Table 3.

 τ_{rep}

For nonsticky polymers, theory predicts⁴⁸

$$\tau_{rep} \approx \tau_e \left(\frac{N}{N_e}\right)^3$$
 [16]

For sticky polymers, before the length of chain between entanglements can move, two Pol+Pol-pairs at an entanglement must break. The probability that a Pol+Pol- pair will break at a specific entanglement, relative to all the entanglements on an entire chain, is N_e/f , where f is the total number of stickers on a chain, f = (1-y)N. The probability that two Pol+Pol- pairs will break at a specific entanglement is $(N_e/f)^2$ leading to the relative chain motion depicted in Scheme 2. The relaxation time for this particular form of "correlated reptation" is

$$\tau_{rep} \approx \tau_e \left(\frac{f}{N_e}\right)^2 \left(\frac{N}{N_e}\right)^3 \approx \tau_e (1-y)^2 \left(\frac{N}{N_e}\right)^5$$
 [17]

 τ_{rep} calculated are also close to the experimental values (Table 3). Combining Equations 10, 11 and 17

$$\eta_0 \approx G_0 \tau_{rep} \approx \left[\frac{kT \emptyset_{PEC}}{d^3} \right] \tau_p (1 - y)^3 \frac{N^5}{N_o^3}$$
[18]

Each of the parameters in Equation 18 has been measured (Table 2 for d, y, ϕ_{PEC} and $\tau_p = \tau_{hop}$; Table 3 for N and N_e = 58). The fit to experimental η_o is good considering the simplicity of the theory (see Figure 7). It is apparent that the scaling of $\eta_o \sim N^5$ is slightly off, and $\eta_o \sim N^{5.4}$ would be a better fit. The slightly larger scaling exponent is assumed to have the same basis (a combination of tube length fluctuations and constraint release⁶⁰) as the $\eta_o \sim N^{3.4}$ experimental for entangled nonsticky polymers.⁵⁹

If for Pair \mathbf{B} (N = 627)

$$D_{pol,rep} \approx \frac{R^2}{\tau_{rep}}$$
 [19]

and $R = \sqrt{6}R_g$ the diffusion coefficient $D_{pol,rep}$ for a chain escaping from its tube is 6 x 10⁻¹⁴ cm² s⁻¹. For a measurement time less than the 200 s reptation time, the migration of one particular chain segment tracked in real time would appear to be subdiffusive.⁶¹

Recent work by the Helm group⁶² shows strong nonlinear scaling of diffusion of a single molar mass deuterated PSS indirectly controlled by PDADMA of various molecular weights, M (a scaling between $D_{PSS} \sim M_{PDADMAC}^{-4.7}$ and $D_{PSS} \sim M_{PDADMAC}^{-7.0}$) in the entangled regime, depending on the preparation conditions, higher than observed⁴⁸ for entangled neutral polymers ($D_{pol} \sim M^{-2}$), and higher than the scaling that might be expected here ($D_{pol} \sim M^{-4.4}$). Under the conditions used (1 M NaCl, room temperature) PDADMA/PSS is close to its glass transition, T_g ,⁶³ whereas PMAPTA/PMA is above T_g (if there is one) at all [NaCl] used here. With polymers having a chemical composition closer to that used here, poly(dimethylaminoethyl methacrylate), PDAMA, and PMANa, D_{pol} was found to scale with M-1, expected for polymers in the overlapped but

unentangled regime.⁶⁴ Given the relatively low M of the PDAMA (30 kg mol⁻¹) and PMA (7 – 480 kg mol⁻¹) used, and the high salt concentration (0.6 M NaCl), that system appears to be in the unentangled regime.

Saloplasticity and Salt Shifting

According to Table 3 and Scheme 1 the salt doping level controls the number of sticky interactions, *f*, per chain according to

$$f = N(1 - y) \tag{20}$$

but the movement of a salt ion in Scheme 1 does not lead to net displacement of polymer segments

Viscoelastic properties of PEC Pair **B** ($n_{avg} = 3730$) in different [NaCl] are shown in Supporting Information Figure S13. To verify that this particular pair was as close to stoichiometric as possible, the ion content was measured with radiolabeled cations ($^{22}Na^{+}$) and anions ($^{35}SO_{4}^{2-}$). The PEC had a 0.4% excess of PMAPTAC, i.e. the stoichiometry was 1.000:1.004 PMA:PMAPTA.

Salt doping effectively shifted the viscoelastic response to lower frequency. $^{20, 25, 54, 56}$ This shift was combined with time-temperature superposition to yield time-temperature-salt superposition shown in Figure 8. The shift factors for this operation, a_s , b_s are given in Supporting Information Figure S7. The rationale behind salt shifting is much less evident than temperature shifting: while there have been attempts to ascribe salt shifting to a decrease in an electrostatic energy barrier due to salt "screening," $^{20, 54, 56}$ it is clear from Equation 18 that several parameters may change with changing [NaCl]. In addition to a decrease in the number of stickers f (by doping according to Equation 1), the volume fraction of polymer changes (see Table 2), as does τ_p , d and

N_e. The a_s shift factor can be broken down into respective individual contributions as follows: a_s = $a_{s,f} \cdot a_{s,\phi} \cdot a_{s,rp} \cdot a_{s,d} \cdot a_{s,Ne}$.

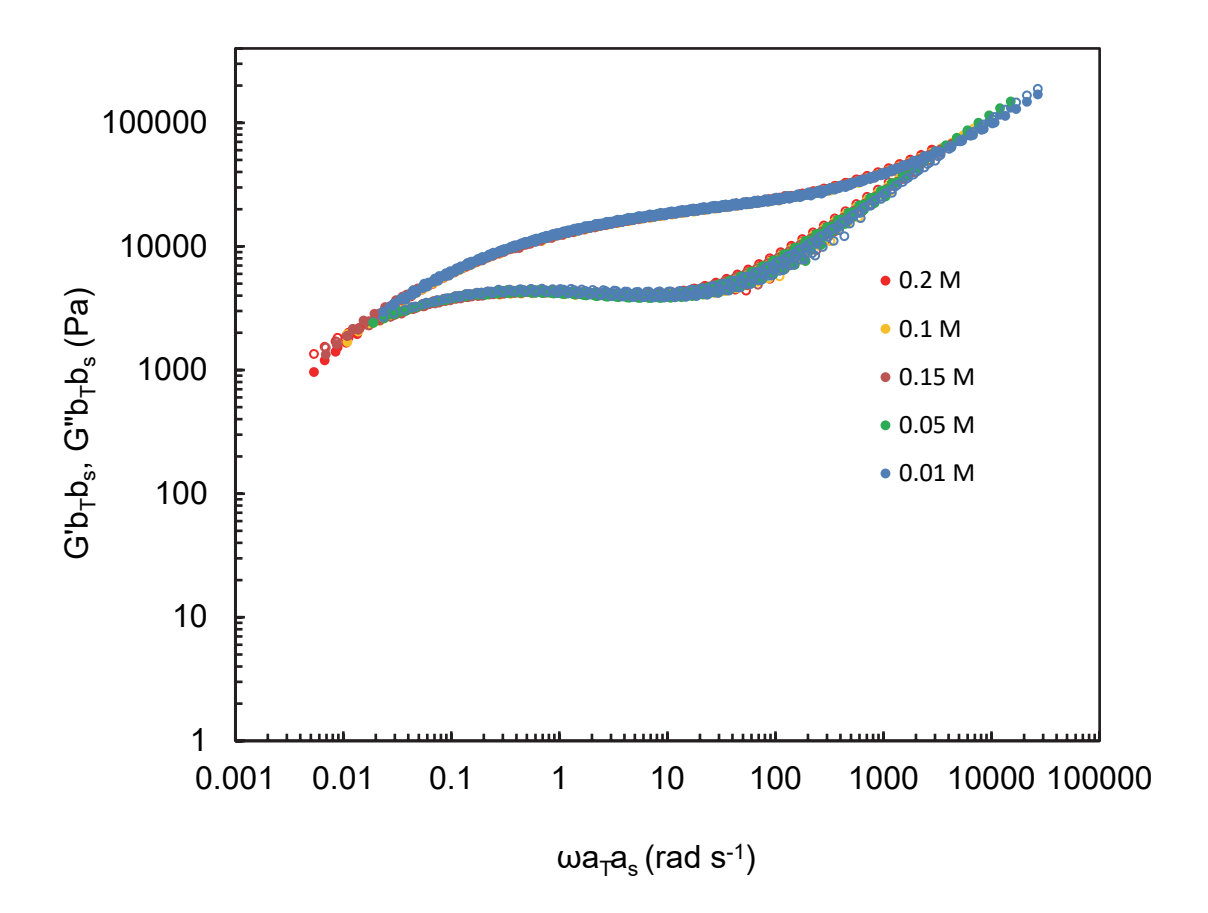


Figure 8. Time-temperature-salt superposition (TTSS) of PMAPTA/PMA PEC Pair **B** (n_{avg} = 3730). Frequencies are shifted along the frequency axis by a temperature factor a_T and a salt factor a_S . Small shifts in the modulus axis, corresponding factors b_T and b_S , are also used. The reference temperature is 25 °C and the reference salt concentration is 0.01M NaCl.

Measured G_0 and relaxation times and calculated zero shear viscosity for Pair **B**, n_{avg} = 3730, in different [NaCl] are summarized in Table 4

Table 4. Plateau modulus, characteristic relaxation times, and activation energies for TTTS for PEC Pair **B** ($n_{avg} = 3730$) at various salt concentrations.

[NaCl] M	0.01	0.05	0.1	0.15	0.2
G ₀ (kPa)	26.3	21.7	25.1	19.2	19.4
Trep (S)	200	175	107	90.1	59.0
τe (S)	1.32 x 10 ⁻³	8.75 x 10 ⁻⁴	4.28 x 10 ⁻⁴	2.50 x 10 ⁻⁴	2.20 x 10 ⁻⁴
$\tau_q(s)$	1.13 x 10 ⁻⁴	-	-	-	-
E _a (kJ mol ⁻¹) ^a	45	43	39	39	38
2E _{open} (kJ mol ⁻¹) ^b	42	41	39	37	37

^aobtained from shift factors and Equation 9.

The dependence of viscosity on salt doping depends on many factors which change, including the cube of the number of stickers (\sim (1-y)³), d³ and ϕ . At present, there is no prediction of how τ_p decreases with salt concentration. However, good experimental estimates for these parameters are provided in Tables 2 and 4. Viscosities predicted by Eq 18 are presented Figure 9.

^bfrom Table 2.

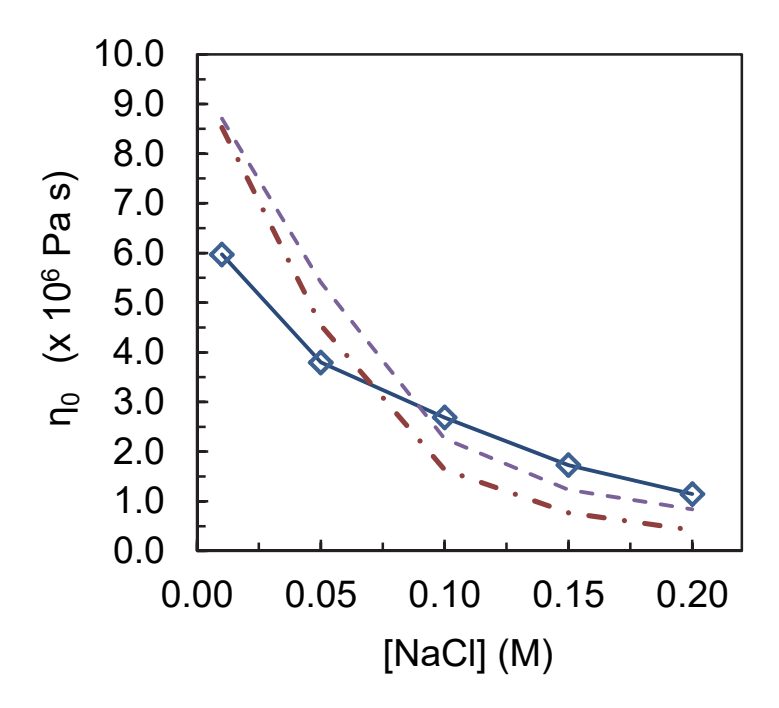


Figure 9. Dependence of viscosity on [NaCl] for PMAPTA/PMA PEC pair B (N = 587). Temperature = 25 °C. \Diamond , measured using η = $G_0\tau_{\rm rep}$ (Table 4); - •, calculated using Equation 18 and values for y, d, ϕ , $\tau_{\rm p}$ from Table 2 and N_e = 58; - - -, calculated using Equation 18 but assuming each mole of NaCl doped into the PEC breaks $\frac{1}{2}$ a mole of crosslinks.

The predicted viscosity starts a little higher but falls faster than experimental in this non-logarithmic plot (Figure 9). As discussed recently, the assumption that one NaCl doped into the PEC breaks one Pol+Pol- pair may not hold for higher levels of doping, since doping itself opens up more free volume for ions to occupy and localizing ions as counterions carries an entropic penalty. In Figure 9 the calculated viscosity assuming only half the NaCl introduced breaks a Pol+Pol- pair gives a better fit at higher [NaCl]. Clearly, the role of ions as counter- or co-ions must be more clearly evaluated for a better description of saloplasticity.

 E_{act} for quadrupolar pair exchange should be twice E_{open} for one Pol⁺Pol⁻ pair breaking (from Table 2). $2E_{open}$ values tabulated in Table 4 are in good agreement with activation energies from shift factors (Equation 9).

Conclusions

This study was enabled by preparing entangled polyelectrolyte complexes with defined composition and properties. To this end, careful fractionation provided individual positive and negative components with high molecular weight and low polydispersity. The stoichiometry of PECs made from select pairs of polyelectrolytes was verified to be close to 1:1. The composition of PECs doped to various levels of salt content was also accurately measured.

Some PECs used previously, such as PDADMA/PSS, have T_g close to room temperature. PMAPTA/PMA, if it has a T_g, must be significantly above T_g in all experiments here, which enabled efficient TTS of all PEC pairs and the use of Arrhenius plots such as the one in Figure S7 Supporting Information. For the first time, LVE measurements captured the entire rubbery plateau for narrow Đ PECs. As expected, the plateau modulus was independent of molecular weight. Entanglement and reptation relaxation times were identified in the LVE, as well as a new relaxation time attributed to pair exchange between two pairs of Pol*Pol*. The "monomer" relaxation time, the fastest, was deduced from ion transport measurements of diffusion coefficient. Because of "sticky" interactions, all relaxation times were slowed compared to nonsticky systems. In addition, the reptation time was unusually slowed, which gives rise to a (zero shear) viscosity that scales with (chain length)⁵. Consideration of the influence of sticky interactions on relaxation lifetimes lead to a new quantitative expression for viscosity that described the data well.

The agreement of experimental versus predicted viscosity for doped PECs as a function of salt concentration was not as good. The instantaneous fraction of salt in PEC that is actually contributing to Pol+Pol- pair breaking as counterions is unknown, which means the total number of stickers is an unknown function of doping. The fraction of counterions is a difficult parameter to measure experimentally, although well-designed NMR experiments may be able to shed light on this question. Molecular dynamics could also provide insight.

The properties of coacervates are dictated by a number of design parameters, many investigated here, including lifetime/strength of stickers, sticker density, chain length, as well as monomer sequence. Additional parameters, available in natural and synthetic polymers, include the structure of the repeat unit, hydrogen bonding and hydrophobic interactions. It would also be interesting to compare PECs with mismatched degrees of polymerization in order to find out whether the properties are averaged or biased towards lighter or heavier chains.

The topic of PEC dynamics is a subset of the broader field of dynamics within soft materials with multiple interactions: each interaction has a characteristic relaxation time, so dynamics must be governed, as they are here, by a strongly nonlinear function of the total number of interactions per molecule. Interactions between polyelectrolytes in PECs are comparable to those between charged polymers and oppositely-charged walls, such as nanopores^{65, 66} for controlled sieving of DNA strands, or thin films of complexed polymers for recognition using nanopores.⁶⁷ In each case, the transport rate of charged polymer should be a strong function of the number of "stickers," which can be based on hydrogen bonding or charge pairing or a combination of both.

Supporting Information

SEC chromatograms of PMAPTAC and PMANa with molecular weights and distributions; photograph of a PEC; NMRs of PECs dissolved in 1.0 M KBr in D_2O ; salt concentration versus time for NaCl release for PECs doped to different levels of y; isothermal calorimetry of PMAPTAC complexing with PMANa; TTS plots of undoped PECs; shift factors for TTS; TTSS plots of pair B ($n_{avg} = 3730$) doped with different salt concentrations; shift factors for TTSS; Arrhenius plots of shift factors versus temperature⁻¹.

Acknowledgment

A portion of this research used resources at the Spallation Neutron Source, a DOE Office of Science User Facility operated by the Oak Ridge National Laboratory (ORNL). This work benefited from the use of the SasView application, originally developed under NSF award DMR-0520547. SasView contains code developed with funding from the European Union's Horizon 2020 research and innovation program under the SINE2020 project, grant agreement No 654000. The authors are grateful for help with neutron scattering provided by Changwoo Do and Volker Urban at ORNL. This research was supported in part by the National Science Foundation, Grant DMR1809304.

References

- 1. Shin, Y.; Brangwynne, C. P. Liquid Phase Condensation in Cell Physiology and Disease. *Science* **2017**, *357*, eaaf4382.
- 2. Bixler, H. J.; Michaels, A. S. Polyelectrolyte Complexes. In *Encyclopedia of Polymer Science and Technology*; Interscience: New York, 1969; Vol. 10, pp 765-80.
- 3. Fuoss, R. M.; Sadek, H. Mutual Interaction of Polyelectrolytes. *Science* **1949**, *110*, 552-4.
- 4. Crowe, C. D.; Keating, C. D. Liquid-Liquid Phase Separation in Artificial Cells. *Interface Focus* **2018**, *8*, 20180032.
- 5. Koga, S.; Williams, D. S.; Perriman, A. W.; Mann, S. Peptide–Nucleotide Microdroplets as a Step Towards a Membrane-Free Protocell Model. *Nat. Chem.* **2011**, *3*, 720-724.
- 6. Poudyal, R. R.; Pir Cakmak, F.; Keating, C. D.; Bevilacqua, P. C. Physical Principles and Extant Biology Reveal Roles for RNA-Containing Membraneless Compartments in Origins of Life Chemistry. *Biochemistry* **2018**, *57*, 2509-2519.
- 7. Mason, A. F.; Yewdall, N. A.; Welzen, P. L. W.; Shao, J.; van Stevendaal, M.; van Hest, J. C. M.; Williams, D. S.; Abdelmohsen, L. K. E. A. Mimicking Cellular Compartmentalization in a Hierarchical Protocell through Spontaneous Spatial Organization. *ACS Central Science* **2019**, *5*, 1360-1365.
- 8. Anderson, D. E.; Becktel, W. J.; Dahlquist, F. W. Ph-Induced Denaturation of Proteins: A Single Salt Bridge Contributes 3-5 kCal/Mol to the Free Energy of Folding of T4 Lysozyme. *Biochemistry* **1990**, *29*, 2403-2408.
- 9. Wang, J.; Scheibel, T. Coacervation of the Recombinant Mytilus Galloprovincialis Foot Protein-3b. *Biomacromolecules* **2018**, *19*, 3612-3619.
- 10. Stewart, R. J.; Wang, C. S.; Song, I. T.; Jones, J. P. The Role of Coacervation and Phase Transitions in the Sandcastle Worm Adhesive System. *Adv Colloid Interfac* **2017**, *239*, 88-96.
- 11. Aumiller, W. M.; Keating, C. D. Phosphorylation-Mediated RNA/Peptide Complex Coacervation as a Model for Intracellular Liquid Organelles. *Nat Chem* **2016**, *8*, 129-137.
- 12. Aumiller, W. M.; Cakmak, F. P.; Davis, B. W.; Keating, C. D. RNA-Based Coacervates as a Model for Membraneless Organelles: Formation, Properties, and Interfacial Liposome Assembly. *Langmuir* **2016**, *32*, 10042-10053.
- 13. Brangwynne, C. P.; Tompa, P.; Pappu, R. V. Polymer Physics of Intracellular Phase Transitions. *Nat Phys* **2015**, *11*, 899-904.

- 14. Lytle, T. K.; Chang, L.-W.; Markiewicz, N.; Perry, S. L.; Sing, C. E. Designing Electrostatic Interactions Via Polyelectrolyte Monomer Sequence. *ACS Central Science* **2019**, *5*, 709-718.
- 15. Wang, J.; Choi, J.-M.; Holehouse, A. S.; Lee, H. O.; Zhang, X.; Jahnel, M.; Maharana, S.; Lemaitre, R.; Pozniakovsky, A.; Drechsel, D.; Poser, I.; Pappu, R. V.; Alberti, S.; Hyman, A. A. A Molecular Grammar Governing the Driving Forces for Phase Separation of Prion-Like RNA Binding Proteins. *Cell* **2018**, *174*, 688-699.e16.
- 16. Sing, C. E. Development of the Modern Theory of Polymeric Complex Coacervation. *Adv Colloid Interfac* **2017**, *239*, 2-16.
- 17. Lou, J.; Friedowitz, S.; Qin, J.; Xia, Y. Tunable Coacervation of Well-Defined Homologous Polyanions and Polycations by Local Polarity. *ACS Central Science* **2019**, *5*, 549-557.
- 18. Li, L.; Srivastava, S.; Andreev, M.; Marciel, A. B.; de Pablo, J. J.; Tirrell, M. V. Phase Behavior and Salt Partitioning in Polyelectrolyte Complex Coacervates. *Macromolecules* **2018**, *51*, 2988-2995.
- 19. Jaber, J. A.; Schlenoff, J. B. Dynamic Viscoelasticity in Polyelectrolyte Multilayers: Nanodamping. *Chemistry of Materials* **2006**, *18*, 5768-5773.
- 20. Spruijt, E.; Cohen Stuart, M. A.; van der Gucht, J. Linear Viscoelasticity of Polyelectrolyte Complex Coacervates. *Macromolecules* **2013**, *46*, 1633-1641.
- 21. Spruijt, E.; Leermakers, F. A. M.; Fokkink, R.; Schweins, R.; van Well, A. A.; Cohen Stuart, M. A.; van der Gucht, J. Structure and Dynamics of Polyelectrolyte Complex Coacervates Studied by Scattering of Neutrons, X-Rays, and Light. *Macromolecules* **2013**, *46*, 4596-4605.
- 22. Wang, Q. F.; Schlenoff, J. B. The Polyelectrolyte Complex/Coacervate Continuum. *Macromolecules* **2014**, *47*, 3108-3116.
- 23. Liu, Y.; Momani, B.; Winter, H. H.; Perry, S. L. Rheological Characterization of Liquid-to-Solid Transitions in Bulk Polyelectrolyte Complexes. *Soft Matter* **2017**.
- 24. Hamad, F. G.; Chen, Q.; Colby, R. H. Linear Viscoelasticity and Swelling of Polyelectrolyte Complex Coacervates. *Macromolecules* **2018**.
- 25. Marciel, A. B.; Srivastava, S.; Tirrell, M. V. Structure and Rheology of Polyelectrolyte Complex Coacervates. *Soft Matter* **2018**, *14*, 2454-2464.
- 26. Huang, J.; Morin, F. J.; Laaser, J. E. Charge-Density-Dominated Phase Behavior and Viscoelasticity of Polyelectrolyte Complex Coacervates. *Macromolecules* **2019**, *52*, 4957-4967.
- 27. Michaels, A. S. Polyelectrolyte Complexes. *Journal of Industrial and Engineering Chemistry* **1965,** *57*, 32-40.
- 28. Bucur, C. B.; Sui, Z.; Schlenoff, J. B. Ideal Mixing in Polyelectrolyte Complexes and Multilayers: Entropy Driven Assembly. *Journal of the American Chemical Society* **2006**, *128*, 13690-13691.
- 29. Schlenoff, J. B.; Yang, M.; Digby, Z. A.; Wang, Q. Ion Content of Polyelectrolyte Complex Coacervates and the Donnan Equilibrium. *Macromolecules* **2019**, *52*, 9149-9159.
- 30. Kumar, R. K.; Harniman, R. L.; Patil, A. J.; Mann, S. Self-Transformation and Structural Reconfiguration in Coacervate-Based Protocells. *Chemical Science* **2016**, *7*, 5879-5887.
- 31. Li, P. L.; Banjade, S.; Cheng, H. C.; Kim, S.; Chen, B.; Guo, L.; Llaguno, M.; Hollingsworth, J. V.; King, D. S.; Banani, S. F.; Russo, P. S.; Jiang, Q. X.; Nixon, B. T.; Rosen, M. K. Phase Transitions in the Assembly of Multivalent Signalling Proteins. *Nature* **2012**, *483*, 336-U129.
- 32. Wang, J. T.; Smith, J.; Chen, B.-C.; Schmidt, H.; Rasoloson, D.; Paix, A.; Lambrus, B. G.; Calidas, D.; Betzig, E.; Seydoux, G. Regulation of Rna Granule Dynamics by Phosphorylation of Serine-Rich, Intrinsically Disordered Proteins in C. Elegans. *eLife* **2014**, *3*, e04591.
- 33. Fu, J.; Fares, H. M.; Schlenoff, J. B. Ion-Pairing Strength in Polyelectrolyte Complexes. *Macromolecules* **2017**, *50*, 1066-1074.
- 34. Choi, U. H.; Ye, Y.; Salas de la Cruz, D.; Liu, W.; Winey, K. I.; Elabd, Y. A.; Runt, J.; Colby, R. H. Dielectric and Viscoelastic Responses of Imidazolium-Based Ionomers with Different Counterions and Side Chain Lengths. *Macromolecules* **2014**, *47*, 777-790.

- 35. Ostendorf, A.; Schönhoff, M.; Cramer, C. Ionic Conductivity of Solid Polyelectrolyte Complexes with Varying Water Content: Application of the Dynamic Structure Model. *Physical Chemistry Chemical Physics* **2019**, *21*, 7321-7329.
- 36. Yang, M.; Shi, J.; Schlenoff, J. B. Control of Dynamics in Polyelectrolyte Complexes by Temperature and Salt. *Macromolecules* **2019**, *52*, 1930-1941.
- 37. Gummel, J.; Cousin, F.; Boue, F. Counterions Release from Electrostatic Complexes of Polyelectrolytes and Proteins of Opposite Charge: A Direct Measurement. *Journal of the American Chemical Society* **2007**, *129*, 5806-5807.
- 38. Spruijt, E.; Westphal, A. H.; Borst, J. W.; Cohen Stuart, M. A.; van der Gucht, J. Binodal Compositions of Polyelectrolyte Complexes. *Macromolecules* **2010**, *43*, 6476-6484.
- 39. Qin, J.; Priftis, D.; Farina, R.; Perry, S. L.; Leon, L.; Whitmer, J.; Hoffmann, K.; Tirrell, M.; de Pablo, J. J. Interfacial Tension of Polyelectrolyte Complex Coacervate Phases. *ACS Macro Letters* **2014**, *3*, 565-568.
- 40. Schlenoff, J. B.; Ly, H.; Li, M. Charge and Mass Balance in Polyelectrolyte Multilayers. *Journal of the American Chemical Society* **1998**, *120*, 7626-7634.
- 41. Helfferich, F. G. *Ion Exchange*; McGraw-Hill: New York,, 1962. p 624 p.
- 42. Dubois, E.; Boue, F. Conformation of Poly(Styrenesulfonate) Polyions in the Presence of Multivalent Ions: Small-Angle Neutron Scattering Experiments. *Macromolecules* **2001**, *34*, 3684-3697.
- 43. Gummel, J.; Boue, F.; Deme, B.; Cousin, F. Charge Stoichiometry inside Polyelectrolyte-Protein Complexes: A Direct Sans Measurement for the Pssna-Lysozyme System. *J. Phys. Chem. B* **2006**, *110*, 24837-24846.
- 44. Gummel, J.; Cousin, F.; Boue, F. Structure Transition in Pss/Lysozyme Complexes: A Chain-Conformation-Driven Process, as Directly Seen by Small Angle Neutron Scattering. *Macromolecules* **2008**, *41*, 2898-2907.
- 45. Chodankar, S.; Aswal, V. K.; Kohlbrecher, J.; Vavrin, R.; Wagh, A. G. Structural Study of Coacervation in Protein-Polyelectrolyte Complexes. *Phys Rev E* **2008**, *78*.
- 46. Markarian, M. Z.; Hariri, H. H.; Reisch, A.; Urban, V. S.; Schlenoff, J. B. A Small-Angle Neutron Scattering Study of the Equilibrium Conformation of Polyelectrolytes in Stoichiometric Saloplastic Polyelectrolyte Complexes. *Macromolecules* **2012**, *45*, 1016-1024.
- 47. Fares, H. M.; Ghoussoub, Y. E.; Delgado, J. D.; Fu, J.; Urban, V. S.; Schlenoff, J. B. Scattering Neutrons Along the Polyelectrolyte Complex/Coacervate Continuum. *Macromolecules* **2018**, *51*, 4945-4955.
- 48. Rubinstein, M.; Colby, R. H. *Polymer Physics*; Oxford University Press: New York, 2003.
- 49. Crank, J. *The Mathematics of Diffusion*; Clarendon Press: Oxford, 1975.
- 50. Crank, J.; Park, G. S. *Diffusion in Polymers*; Academic Press: London, New York,, 1968. p xii, 452 p.
- 51. Middleton, L. R.; Winey, K. I. Nanoscale Aggregation in Acid- and Ion-Containing Polymers. *Annual Review of Chemical and Biomolecular Engineering* **2017**, *8*, 499-523.
- 52. Abhyankar, N.; Ghoussoub, Y. E.; Wang, Q.; Dalal, N. S.; Schlenoff, J. B. Ion Environments in Mn²⁺-Doped Polyelectrolyte Complexes: Dilute Magnetic Saloplastics. *The Journal of Physical Chemistry B* **2016**, *120*, 6771-6777.
- 53. Decher, G. Fuzzy Nanoassemblies: Toward Layered Polymeric Multicomposites. *Science* **1997**, 277, 1232-1237.
- 54. Spruijt, E.; Sprakel, J.; Lemmers, M.; Stuart, M. A. C.; van der Gucht, J. Relaxation Dynamics at Different Time Scales in Electrostatic Complexes: Time-Salt Superposition. *Physical Review Letters* **2010**, *105*, 208301.
- 55. Liu, Y. L.; Winter, H. H.; Perry, S. L. Linear Viscoelasticity of Complex Coacervates. *Adv Colloid Interfac* **2017**, *239*, 46-60.

- 56. Ali, S.; Prabhu, V. Relaxation Behavior by Time-Salt and Time-Temperature Superpositions of Polyelectrolyte Complexes from Coacervate to Precipitate. *Gels* **2018**, *4*, 11.
- 57. Fares, H. M.; Wang, Q.; Yang, M.; Schlenoff, J. B. Swelling and Inflation in Polyelectrolyte Complexes. *Macromolecules* **2019**, *52*, 610-619.
- 58. Rubinstein, M.; Semenov, A. N. Dynamics of Entangled Solutions of Associating Polymers. *Macromolecules* **2001**, *34*, 1058-1068.
- 59. Colby, R. H.; Fetters, L. J.; Graessley, W. W. The Melt Viscosity-Molecular Weight Relationship for Linear Polymers. *Macromolecules* **1987**, *20*, 2226-2237.
- 60. Likhtman, A. E.; McLeish, T. C. B. Quantitative Theory for Linear Dynamics of Linear Entangled Polymers. *Macromolecules* **2002**, *35*, 6332-6343.
- 61. Kienle, D. F.; Schwartz, D. K. Complex Salt Dependence of Polymer Diffusion in Polyelectrolyte Multilayers. *The Journal of Physical Chemistry Letters* **2019**, *10*, 987-992.
- 62. Sill, A.; Nestler, P.; Azinfar, A.; Helm, C. A. Tailorable Polyanion Diffusion Coefficient in Lbl Films: The Role of Polycation Molecular Weight and Polymer Conformation. *Macromolecules* **2019**, *52*, 9045-9052.
- 63. Shamoun, R. F.; Hariri, H. H.; Ghostine, R. A.; Schlenoff, J. B. Thermal Transformations in Extruded Saloplastic Polyelectrolyte Complexes. *Macromolecules* **2012**, *45*, 9759-9767.
- 64. Xu, L.; Selin, V.; Zhuk, A.; Ankner, J. F.; Sukhishvili, S. A. Molecular Weight Dependence of Polymer Chain Mobility within Multilayer Films. *ACS Macro Letters* **2013**, *2*, 865-868.
- 65. Lin, C.-Y.; Combs, C.; Su, Y.-S.; Yeh, L.-H.; Siwy, Z. S. Rectification of Concentration Polarization in Mesopores Leads to High Conductance Ionic Diodes and High Performance Osmotic Power. *Journal of the American Chemical Society* **2019**, *141*, 3691-3698.
- 66. Eggenberger, O. M.; Ying, C.; Mayer, M. Surface Coatings for Solid-State Nanopores. *Nanoscale* **2019**, *11*, 19636-19657.
- 67. Ali, M.; Yameen, B.; Neumann, R.; Ensinger, W.; Knoll, W.; Azzaroni, O. Biosensing and Supramolecular Bioconjugation in Single Conical Polymer Nanochannels. Facile Incorporation of Biorecognition Elements into Nanoconfined Geometries. *Journal of the American Chemical Society* **2008**, *130*, 16351-16357.

TOC Graphic

